ARTICLE NO. 78-960R

Effects of Airframe-Inlet Integration on Half-Axisymmetric and Two-Dimensional Supersonic Inlet Performance

Lewis E. Surber* and Dennis Sedlock†
Air Force Flight Dynamics Laboratory, Wright Patterson AFB, Ohio

Diagnostic data from large-scale, airframe-inlet model wind-tunnel tests have been analyzed to facilitate understanding of both axisymmetric and two-dimensional inlet performance in different installation configurations of highly maneuverable supersonic aircraft. Distortion pattern shifts have been used to identify duct swirl, apparently due to duct offset and loft. Examinations of total pressure surveys through the ducts of various inlet installations have been used to show the influence of flow separation at the inlet aperture and in the throat on performance degradation in various inlet configurations. Benefits and limitations of inlet shielding in supersonic maneuvering flight have been explored, showing performance advantages of half-axisymmetric inlets over two-dimensional inlets in the wing-shielded flowfields and more general performance advantages associated with fuselage shielding. Data comparisons have incorporated total pressure recovery, duct turbulence, and compressor face steady-state and dynamic flow distortion index showing, in particular, the importance of dynamic flow distortion measurement and sophisticated, high-speed analysis capability.

Nomenclature

M	= Mach number
p	= total pressure
P_{rms}	= root mean square of compressor face total pressure fluctuations (average of all probes)
$\bar{P}_2/P_0$	= pressure recovery (compressor face average total pressure ratioed to freestream total pressure)
$\Delta P_{rms}/\bar{P}_2$	= compressor face total pressure turbulence parameter
K/K_L, K/K_{limit}	= ratio of distortion parameter K_A to its limit value
α	= angle of attack
β	= angle of sideslip‡

Subscripts

0	= freestream value
L	= local value

Introduction

THE inlet/airframe integration problem, basically, is to provide for efficient, uniform delivery of air to the aircraft engine at all operating conditions. In the case of turbine engine aircraft operating in the subsonic/supersonic Mach number range, inlet performance is measured in terms of its effect on both the thermodynamic performance of the engine and the aerodynamic performance of the airframe. This paper focuses on parameters involved in the determination of thermodynamic inlet performance, including total pressure recovery, flow distortion, and turbulence at the engine compressor face. Specifically, it summarizes supplemental analysis of data generated under Project Tailor-Mate, a multiphase program consisting of forebody flowfield and inlet performance investigations.

The objective of the Tailor-Mate program was to generate design guidelines for air superiority aircraft inlets. To that end, models and instrumentation were carefully designed not only to assess the basic inlet performance parameters but also to generate diagnostic information about inlet flowfields. Thus, Tailor-Mate truly created a "data bank" for a wide array of supersonic external compression inlet installations. In the early part of that program, a wide spectrum of fighter aircraft designs were explored. From this array of configurations, the designs of Fig. 1 were selected for the main thrust of the experimental program. Four of the airframe-inlet configurations, i.e., the side-mounted and wing-shielded designs, had a Mach 2.5 design point, but the fuselage-shielded inlet was designed for Mach. 2.2.

All three of the two-dimensional inlet configurations employed horizontal compression ramps. The side-mounted

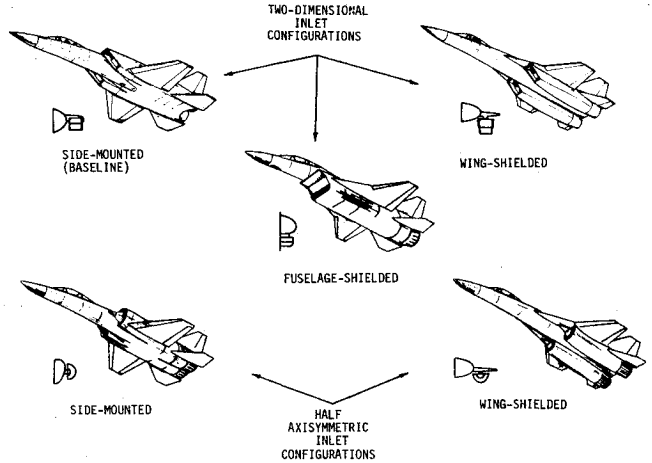

Fig. 1 Tailor-Mate airframe-inlet configurations.

Presented as Paper 78-960 at the AIAA/SAE 14th Joint Propulsion Conference, Las Vegas, Nev., July 25-27, 1978; submitted Oct. 23, 1978; revision received Feb. 1, 1979.

Index categories: Airbreathing Propulsion; Aerodynamics; Performance.

*Aerospace Engineer, Internal Aerodynamics.

†Aerospace Engineer, Internal Aerodynamics. Member AIAA.

‡Positive sideslip is defined as that condition for which the aircraft nose is left and the inlet under consideration is on the leeward side of the fuselage.

and wing-shielded of these two forebody-inlet models used porous-bleed variable second and third compression ramps, along with porous sideplates and a variable-height throat slot for inlet flow control and stabilization. Left-hand inlets incorporated 40 combination steady-state and high-response, total pressure probes. Additional instrumentation was provided in the right-hand inlets, consisting of total pressure rakes and static pressure taps through the duct. The single, Mach 2.2 fuselage-shielded inlet had a variable geometry second ramp with throat slot bleed. Because there was only one duct on this model, the compressor face dynamic pressure instrumentation was employed without the use of upstream diagnostic total pressure rakes.

In the lower part of Fig. 1, the two half-axisymmetric inlet installation configurations are depicted. These inlets shared a common semiconical compression surface with a fixed first cone angle of 18 deg. Porous plate boundary-layer bleed was provided on the second cone of each of these inlets, spanning the region of the normal shock location. Several discrete semicone compression surfaces were fabricated, each being tested in the Mach environment for which it had been designed. Both half-axisymmetric inlets employed high-response and diagnostic instrumentation similar to the side-mounted and wing-shielded two-dimensional inlet installations. Values of duct length to compressor face diameter ratio (L/D) ranged from 5.8 (fuselage-shielded inlet) and 5.2 (side-mounted inlets) down to approximately 3 (wing-shielded inlets).

Previous documentation has included AFFDL technical reports[1-3] and various technical papers.[4,5] Rather than attempt to discuss the full Mach 0.9-2.5 range encompassed by the program, this paper will deal essentially with Mach 2.2 over a wide range of maneuver conditions.

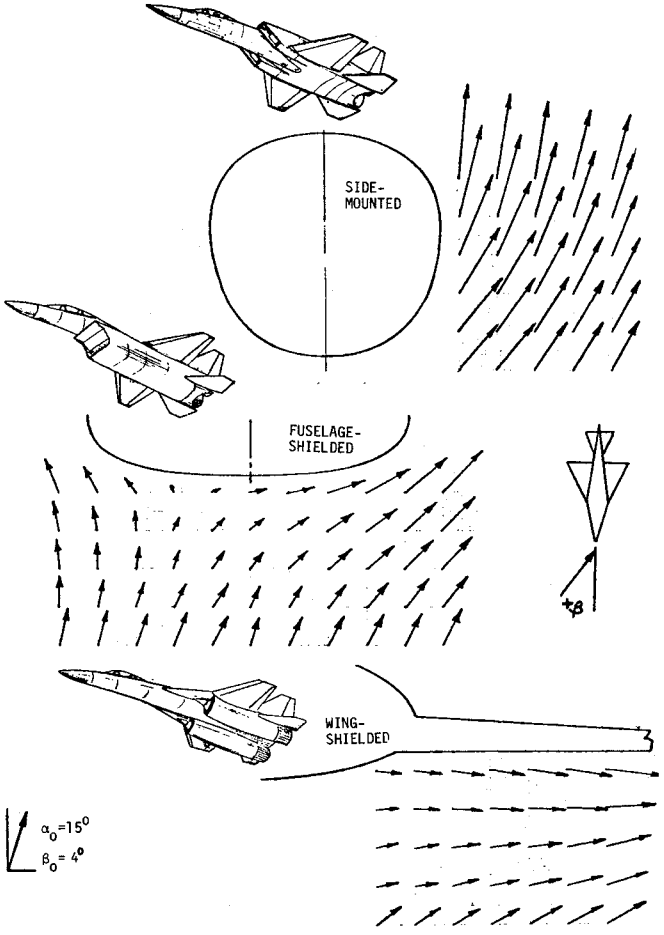

Fig. 2 Comparison of vector flowfields; $M_0=2.2$, $\alpha_0=15$ deg, $\beta_0=4$ deg.

Inlet Environments

Trends of average values of flowfield angularity for the three types of inlet flowfields studied (side-mounted, wing-shielded, fuselage-shielded) suggest that both types of shielded configurations reduce average inlet flowfield local angle of attack ($\bar{\alpha}_L$) in maneuvering flight with the wing-shielded configuration being the most effective. On the other hand, average levels of local sideslip ($\bar{\beta}_L$) are about the same for all three installation types over the -5 deg $\leq \alpha_0 \leq 25$ deg angle-of-attack and -8 deg $\leq \beta_0 \leq +8$ deg angle-of-sideslip ranges.

It becomes necessary to examine details of the flowfield in order to highlight important differences among the three inlet environments. Study of an individual maneuver condition, such as that depicted in the Fig. 2 vector flowfield plots ($M_0=2.2$, $\alpha_0=15$ deg, $\beta_0=4$ deg), make it obvious that flowfield averages alone do not give sufficient information about inlet installation. Although the average levels of sideslip are approximately the same in all three of these cases, the maximum β_L values for the side-mounted installation exist in the region of the lower inboard sideplate, such that there would be a tendency for flow to separate inside the sideplate/cowl. Conversely, maximum sideslip values in the fuselage-shielded installation are in the outboard portion of the flowfield, so that separation would tend to occur outside the inlet sideplate. In the wing-shielded installation as well, maximum values of sideslip occur in the outboard region. Here, however, moderate levels of pure sideslip flow exist inboard as well. Judging from this figure, it may be anticipated that the shielded configurations reduce levels of α_L in maneuvering flight quite effectively, but that this advantage could be tempered for the wing-shielded concept by the existence of moderately high levels of β_L at the inboard sideplate.

Specific Integration Problems

2-D Inlets—Sideplate Flow Distortion

Figure 3 shows the effect of the $M_0=2.2$, $\alpha_0=15$ deg, $\beta_0=4$ deg flow environment on the side-mounted and wing-shielded two-dimensional inlet internal flows by means of contours of local total pressure ratioed to freestream total pressure. Immersed in the flowfield depicted in Fig. 2, the side-mounted inlet experiences extensive flow separation on the inboard sideplate at the cowl lip station. The separation and its effects have spread significantly at the throat and continue to spread in the duct. Note that the region of highest energy air appears to migrate upward as flow progresses through the duct so that at the compressor face the very lowest pressures have essentially moved to the bottom half of the duct. With the wing-shielded inlet, it is seen that the cowl lip total pressure profiles are quite similar to the side-mounted inlet, but that there is no shifting of the distortion pattern through the duct. Despite worse throat flow conditions in the side-mounted inlet, its longer duct provides mixing sufficient to reduce turbulence and peak distortion levels below those of the short duct, wing-shielded inlet. Table 1 gives a comparison of the performance of the two inlets at this condition.

Two-Dimensional Inlets—Distortion Pattern Shift

Focusing on the distortion pattern shift noted in the side-mounted inlet total pressure maps in Fig. 3, Fig. 4 presents

Table 1 Inlet performance comparison

	Side-mounted	Wing-shielded
$\bar{P}_2/P_0$	0.731	0.875
$\Delta P_{rms}/\bar{P}_2$	0.026	0.042
K/K_L	0.335	0.942
$(K/K_L)_{peak}$	0.609	1.722

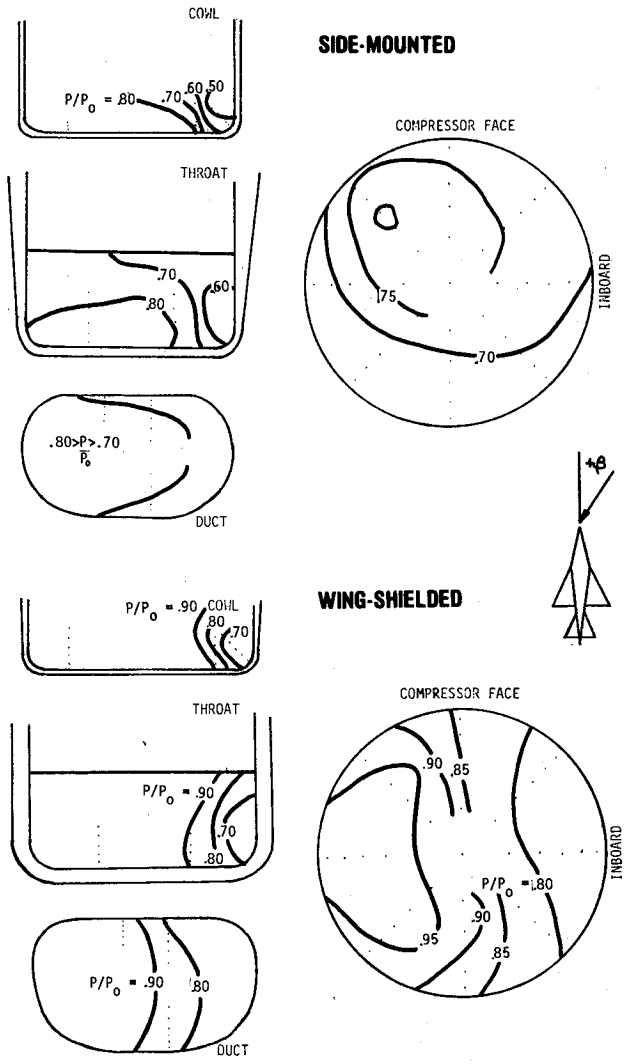

Fig. 3 Inlet total pressure maps; $M_0 = 2.2$, $\alpha_0 = 15$ deg, $\beta_0 = 4$ deg.

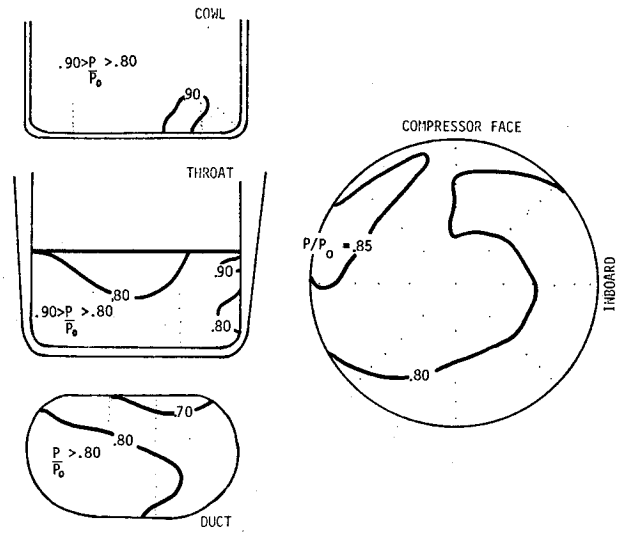

Fig. 4 Inlet total pressure maps, side-mounted two-dimensional inlet; $M_0 = 2.2$, $\alpha_0 = 20$ deg, $\beta_0 = 0$ deg.

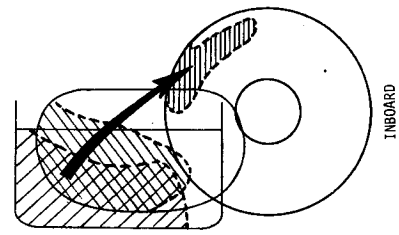

Fig. 5 Apparent progression of high energy flow, side-mounted two dimensional inlet; $M_0 = 2.2$, $\alpha_0 = 20$ deg, $\beta_0 = 0$ deg

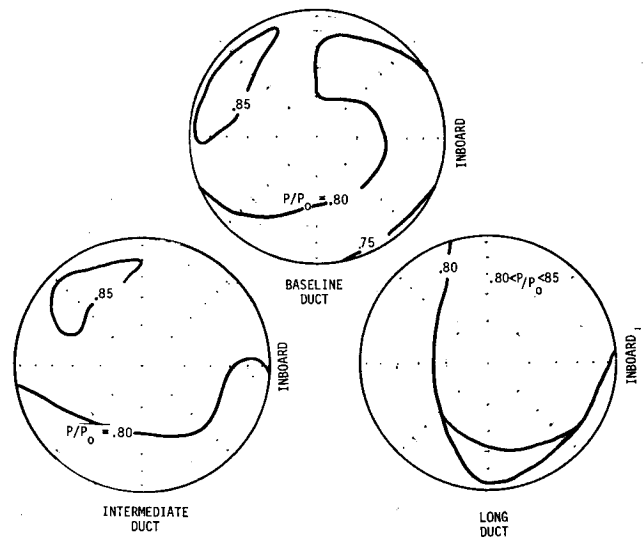

Fig. 6 Side-mounted two-dimensional inlet compressor face plots, duct length comparison; $M_0 = 2.2$, $\alpha_0 = 20$ deg, $\beta_0 = 0$ deg.

similar maps for $\alpha_0 = 20$ deg, $\beta_0 = 0$ deg in order to show that the pattern shift is not caused by model yaw. In this case, movement of the low-energy flow to the inboard and lower part of the inlet still appears to be quite evident. It is hypothesized, then, that the movement of total pressure patterns through the duct is related to inlet offset. Figure 5 shows a superposition of the inlet throat, duct, and compressor face with shaded areas representing regions of high pressure at $\alpha_0 = 20$ deg. As flow progresses through the duct, the mass of air is pushed upward and inboard, apparently inducing a swirling motion. The portion of the throat flow with highest total pressure has slightly higher momentum than the rest of the flowfield. Therefore, its initial movement, as indicated by the arrow, may tend to be the dominant factor in the formation of the compressor face total pressure pattern. In an effort to explore this phenomenon further, data have been examined in which simple cylindrical extensions have been placed between the baseline duct exit and the inlet compressor face instrumentation, increasing duct L/D from 5.23 to 6.58 (intermediate duct) and to 7.94 (long duct). The effect of duct length on the compressor face profiles at $\alpha_0 = 20$ deg is shown in Fig. 6. Note that as the flow progresses through the cylindrical duct section, the high- and low-pressure regions continue to shift or rotate in a clockwise direction. Even at $\alpha_0 = 0$ deg, $\beta_0 = 0$ deg (Fig. 7), duct swirl seems evident as the low-pressure region moves from the seven o'clock position to nine o'clock in the intermediate duct extension and continues to the ten o'clock position in the long duct. Thus, while the basic mechanism of duct swirl can be argued, these data seem to leave no doubt concerning their existence.

Half-Axisymmetric Inlets—
Side-Mounted Inlet Throat Separation at α_0

The half-axisymmetric inlet performs reasonably well at Mach 2.2, $\alpha_0 = 0$ deg, but its performance drops off rapidly with increasing angle of attack. Flow progression through the inlet is shown in Fig. 8 at $\alpha_0 = 0$ and 10 deg in order to shed

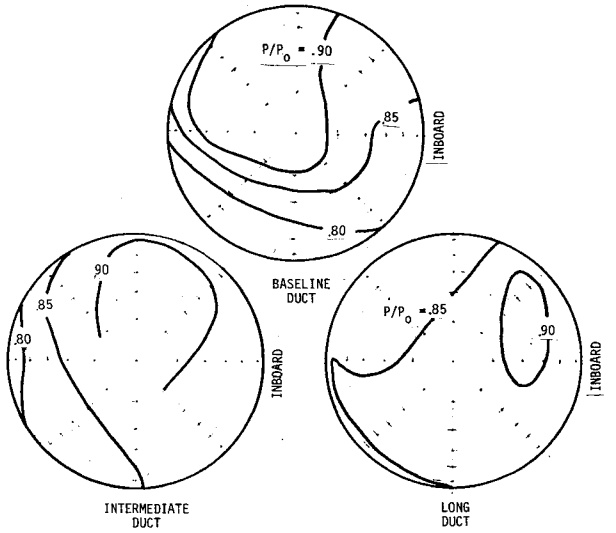

Fig. 7 Side-mounted two-dimensional inlet compressor face plots, duct length comparison; $M_0 = 2.2$, $\alpha_0 = 0$ deg, $\beta_0 = 0$ deg.

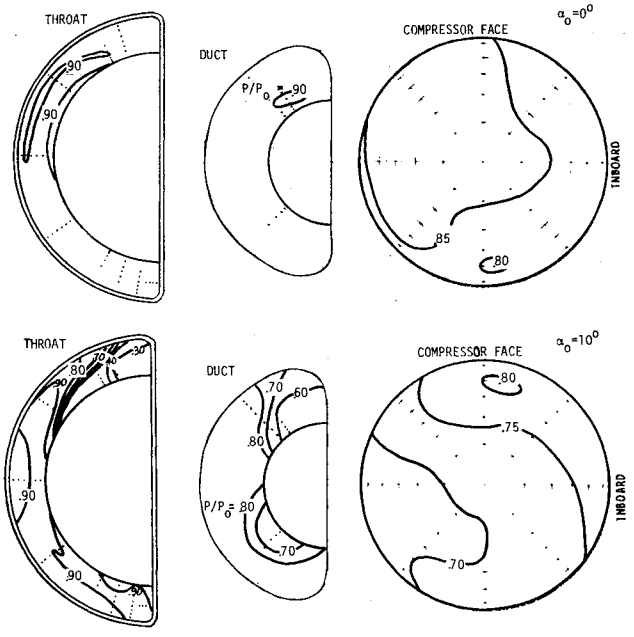

Fig. 8 Side-mounted axisymmetric inlet total pressure maps; $M_0 = 2.2$, $\beta_0 = 0$ deg.

light on the process of flow deterioration. High recovery prevails across the duct all the way to the compressor face at $\alpha_0 = 0$ deg, but at the higher angle of attack, $\alpha_0 = 10$ deg, a massive flow separation originates in the upper part of the inlet throat. Farther down the duct, the flow in this upper region is still separated, but has been joined by a separation region in the lower part of the throat, adjacent to the spike. At the compressor face, evidence of the separated flows is obvious in the low-pressure regions, but it is not clear how the flow has been altered in order to create the compressor face pattern.

Based on the Tailor-Mate investigation, the side-mounted, half-axisymmetric inlet appears to be a poor performer. Yet, several current aircraft systems employ this inlet effectively and it can be attractive from structures, system drag, and reduced observables viewpoints. It was not in the scope of the Tailor-Mate investigation to refine and develop each inlet when problems were discovered, but there are some possibilities for future investigations which these data suggest. First, the fixed geometry compression surfaces were

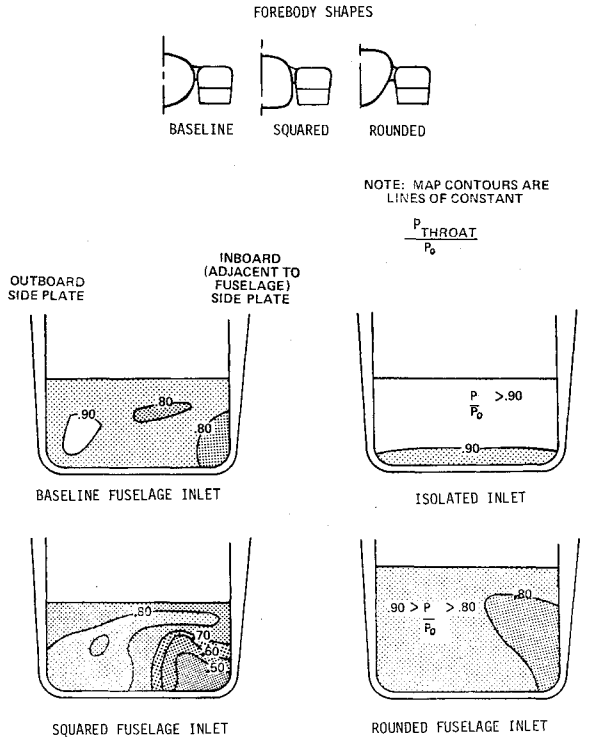

Fig. 9 Side-mounted two-dimensional inlet effect of forebody shape on throat total pressures; $M_0 = 2.2$, $\alpha_0 = 15$ deg, $\beta_0 = 0$ deg.

not amenable to determination of optimum angles, but this type of work should be done. Second, the boundary-layer control system may need to be more sophisticated so that it works efficiently at high angles of attack where it is most needed. As it is, the upper spike surface pressures approach plenum pressures at high α_0, so that the terminal shock in that upper inlet region is quite strong and is impinging on a thick boundary layer. It may also be possible that there is some reverse flow through the bleed holes in this region. Therefore, it might be necessary to employ a type of scoop bleed or plenum compartmenting or both to improve this performance. Third, some type of compression surface α_0-bias may be considered; i.e., variable geometry control to increase cone angle on the upper spike surface and reduce it on the lower surface as angle of attack increases. Of course the considerable complexities of such a system would have to be weighed against the potential advantages very carefully. Finally, care would also have to be taken with this type of an inlet to design the diverter/sideplate carefully enough to avoid the sideplate leading edge separation which occurs with the Tailor-Mate design at α_0.

Taking Advantage of Integration

Two-Dimensional Inlets—Forebody Shaping

Among the techniques available for improving airframe/propulsion integration, fuselage lower shoulder shaping has been found to be of significant importance for side-mounted, two-dimensional inlets. Test data are shown in Fig. 9 for three different forebody cross section shapes, as well as the isolated condition, revealing a definite and substantial effect of forebody shape on maneuvering flight performance. Isolated inlet pressure recovery shows the least sensitivity to α_0, while performance of the inlet integrated with the squared-bottom fuselage shape deteriorates quite sharply above $\alpha_0 = 10$ deg.[3,5] Figure 9 gives an example of the throat flow variations associated with the different forebody influences at $\alpha_0 = 15$ deg. Influence of the forebody is seen in all three integrated configurations, but is, by far, the most prominent with the squared forebody, where a substantial

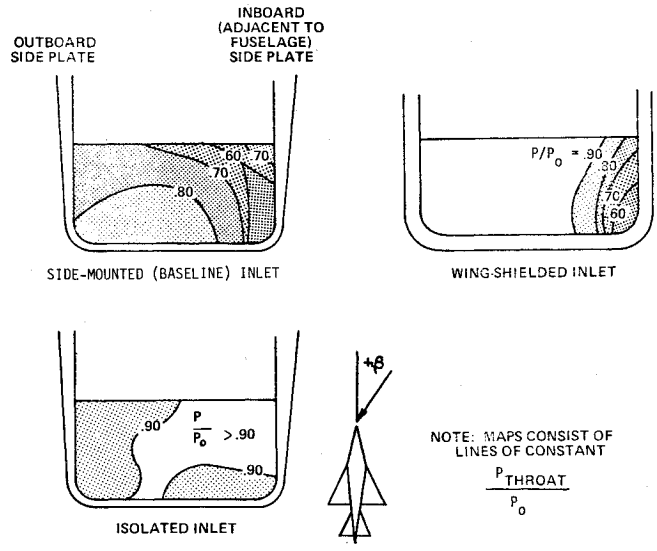

Fig. 10 Inlet total pressure maps for different inlet installation types; $M_0 = 2.2$, $\alpha_0 = 15$ deg, $\beta_0 = 4$ deg.

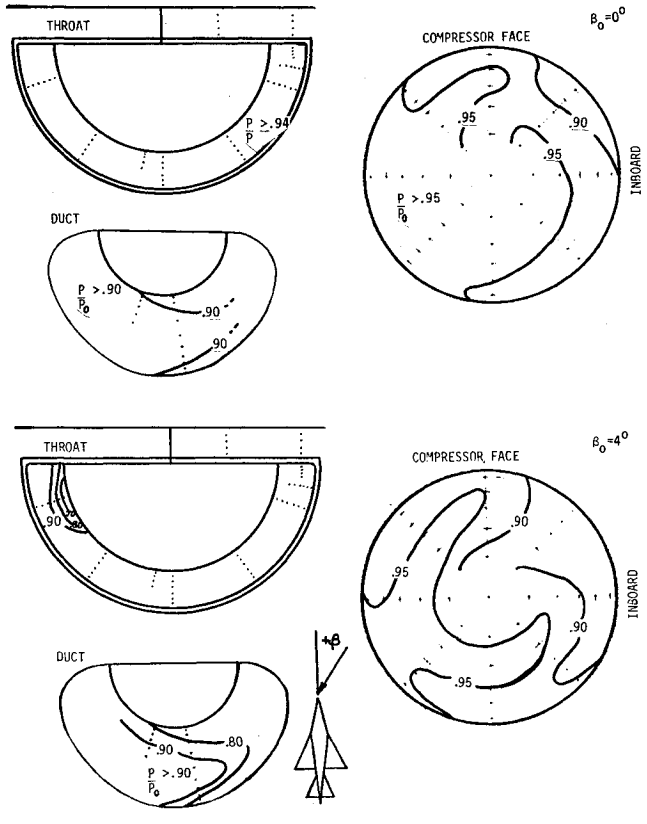

Fig. 11 Wing-shielded axisymmetric inlet total pressure maps; $M_0 = 2.2$, $\alpha_0 = 15$ deg, $\beta_0 = 0$ deg, 4 deg.

region of flow separation dominates the lower inboard region of the throat. Thus, careful rounding of the fuselage lower shoulder of side-mounted inlet configurations can be used to enhance inlet-engine compatibility.

Half-Axisymmetric Inlets—Effect of Wing Shielding

One of the alternatives to the side-mounted inlet installation, in an effort to further improve prospects for compatibility, is to position the inlet under the aircraft wing and take advantge of the inherent shielding from angle of attack. As shown in Fig. 2, however, this can generate about 6 degrees-of-sideslip flow at the inboard side of the inlet

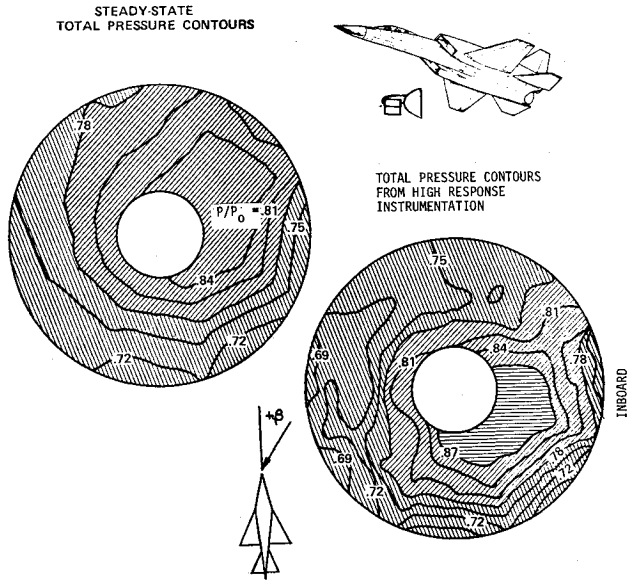

Fig. 12 Compressor face total pressure contours, baseline inlet configuration; $M_0 = 1.6$, $\alpha_0 = 15$ deg, $\beta_0 = 8$ deg.

position. In fact, Fig. 10 shows that both the side-mounted and wing-shielded two-dimensional inlets at $M_0 = 2.2$, $\alpha_0 = 15$ deg, $\beta_0 = 4$ deg, experience severe flow separation at the inboard side of the throat. In both of these cases, the separated throat flow translates to high compressor face flow distortion (see Ref. 3). On the other hand, sideslip flow approaching the inboard side of the leeward wing-shielded, half-axisymmetric inlet is turned into the duct by the centerbody compression spike and, consequently, does not have the same tendency to separate as observed with the wing-shielded, two-dimensional inlet. The flow progression maps of Fig. 11 show that as sideslip reaches $\beta_0 = 4$ deg, a small separation on the outboard (leeward) side of the spike develops, but dissipates in the duct and is not seen at the compressor face. The wing-shielded, half-axisymmetric inlet then reduces angularity effects sufficiently to maintain very good performance coupled with low-flow distortion over a wide range of supersonic maneuver conditions.

Two-Dimensional Inlets—Effect of Fuselage Shielding

Another alternative to the side-mounted inlet installation involves the use of fuselage shielding. As indicated earlier, the centerline placement of the fuselage-shielded inlet provides additional protection for a two-dimensional inlet in that it tends to eliminate the problem of internal flow separation at the inlet sideplate. While no diagnostic duct total pressure data are available for the fuselage-shielded inlet, comparisons of steady-state and "instantaneous" (peak) compressor face total pressure maps for the three different types of two-dimensional inlet installations are shown in Figs. 12-14. These data points are taken from $M_0 = 1.6$, $\alpha_0 = 15$ deg sideslip sensitivity data (see Ref. 3) comparing $\beta_0 = 8$ deg points. For situations where inlet rms turbulence is high, such as the side-mounted and wing-shielded inlets in Figs. 12 and 13 (turbulence greater than 0.03), there is a large difference between the steady-state and maximum peak total pressure patterns. But where there is a low level of compressor face turbulence using the fuselage-shielded inlet (turbulence less than 0.0l), Fig. 14 indicates that the two types of total pressure maps are very similar. Thus, for two-dimensional inlets, only the fuselage-shielded installation consistently retains the benefits of shielding when realistic maneuvers, including yaw, at supersonic Mach numbers are examined. A later section will compare average performance parameters over a range of α_0 and α_0/β_0 conditions to further highlight the points made in this section.

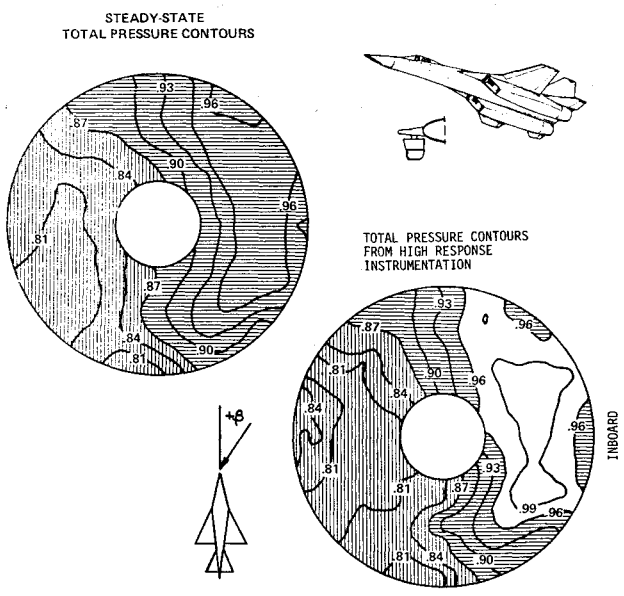

Fig. 13 Compressor face total pressure contours, wing-shielded two-dimensional inlet configuration; $M_0 = 1.6$, $\alpha_0 = 15$ deg, $\beta_0 = 8$ deg.

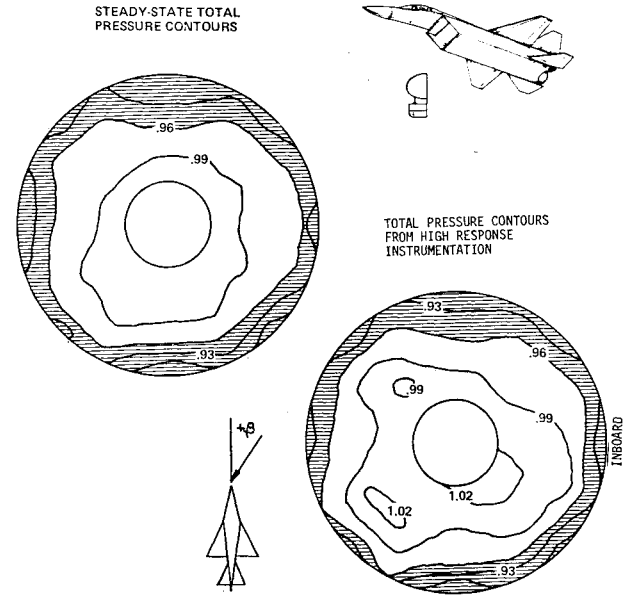

Fig. 14 Compressor face total pressure contours; fuselage-shielded two-dimensional inlet configuration; $M_0 = 1.6$, $\alpha_0 = 15$ deg, $\beta_0 = 8$ deg.

Next, however, the system developed to analyze distortion, as measured by high-response total pressure instrumentation, will be discussed.

Flow Distortion Criteria and Analysis

With over 4000 data points taken during the Tailor-Mate test program, it would have been possible to digitize the compressor face pressure data only for a select number of cases to arrive at peak distortion levels. Fortunately, an analog-editing system, called DYNADEC (Dynamic Data Editing and Computing), had been developed by AFFDL and the ASD Computer Center.[6] The system was developed for the purpose of determining peak distortion levels using engine distortion parameters as the screening criteria. With this system, it became possible to screen significant quantities of analog data for the purpose of assessing inlet-engine compatibility. Analog tapes, containing the compressor face pressure data that are recorded during the test, are played back through a multiplex discriminator system. Each pressure transducer signal is filtered according to model scale size and engine sensitivity. The fluctuating pressures are then combined with their steady-state component on the analog computer (Comcor CI-5000/6) in the appropriate manner to form the engine distortion parameters. A distortion parameter is then fed into a peak detector network. As peaks are detected, the level of the parameters and the time of occurrence are transferred to the digital computer (Xerox Sigma 7). At the conclusion of the data record, a history of peaks is printed via line printer, as well as the pressure distortion map for the maximum peak distortion level. Distortion levels exceeding a limit value provided by the engine manufacturer are then seen to represent a potential inlet-engine compatibility problem. Further analysis is required, of course, to determine if all available surge margin is used by the distortion.

The Tailor-Mate data were screened [7,8] with the Pratt and Whitney engine distortion parameter K_A, the general expression of which is:

$$K_A = K_\theta + bK_{RA}$$

where K_A represents the total distortion and is a weighted sum of the circumferential distortion level, K_θ, and the radial distortion, K_{RA}. A detailed description of these distortion parameters can be found in Ref. 6. Weighting factors and constants used in the solution of the equations were an extension of those developed for the F100-PW-100 specification engine. The use of particular weighting factors does tend to judge inlet-engine compatability in light of a specific engine's sensitivity to circumferential and radial distortion, consequently making the reduced data inappropriate for direct application to more recent builds of the engine. Nevertheless, this approach does allow a relative ranking and comparison of the various inlet-engine installations.

Performance Comparisons: Two-Dimensional vs Axisymmetric

This final section is for the purpose of generating cross-comparisons of two-dimensional and half-axisymmetric inlet performance parameters over a range of angles of attack and angles of sideslip at Mach 2.2.

Total Pressure Recovery

Comparing Mach 2.2 average total pressure recoveries of the five inlet installations in Fig. 15, it is seen that total pressure recovery sensitivity to angle of attack, α_0, and angle of sideslip, β_0, varies greatly. Wing shielding is effective for both two-dimensional and axisymmetric inlets in pure α_0 maneuvers, resulting in high recovery over the 0 deg $\leq \alpha_0 \leq$ 25 deg range. On the other hand, both of the side-mounted inlets exhibit sensitivity to α_0, with the half-axisymmetric inlet performance dropping off rapidly above $\alpha_0 = 0$ deg. Fuselage shielding is also seen to be effective at α_0. The performance decrement of the fuselage-shielded inlet with respect to the wing-shielded inlets at all α_0 is a result of its simpler, single-variable ramp, lower Mach number design.

Looking at the sensitivity of inlet pressure recovery to β_0 at $\alpha_0 = 15$ deg, the performance of all but the fuselage-shielded inlet deteriorate above $\beta_0 = 0$ deg. In fact, of the other four inlets, the performance of all but the wing-shielded half-axisymmetric inlet drop precipitously with positive β_0. Note that this sensitivity includes the wing-shielded, two-dimensional inlet, which produced the highest pressure recovery over the 10 deg $\leq \alpha_0 \leq$ 25 deg range at $\beta_0 = 0$ deg.

Steady-State Flow Distortion

The two-dimensional, wing-shielded inlet is shown in Fig. 16 to be extremely sensitive to negative angle of attack at $\beta_0 = 0$ deg and positive β_0 at $\alpha_0 = 15$ deg in terms of com-

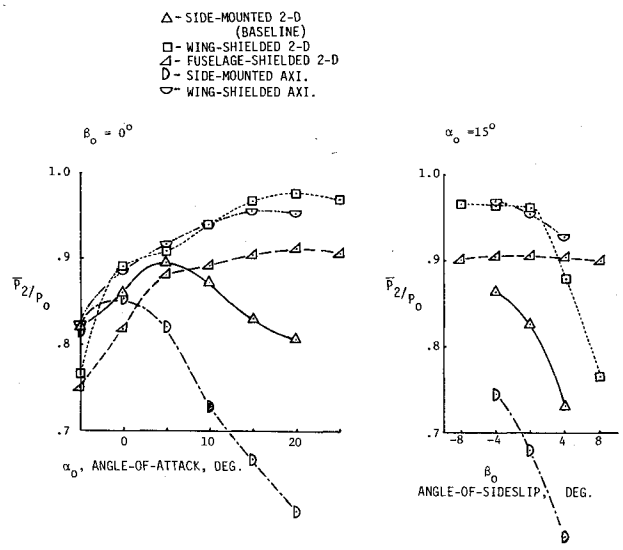

Fig. 15 Comparison of two-dimensional and axisymmetric inlet pressure recovery; $M_0 = 2.2$.

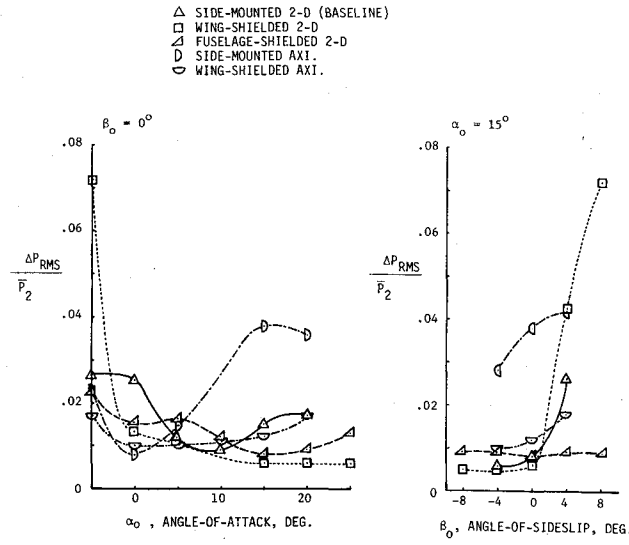

Fig. 17 Comparison of two-dimensional and axisymmetric inlet turbulence; $M_0 = 2.2$.

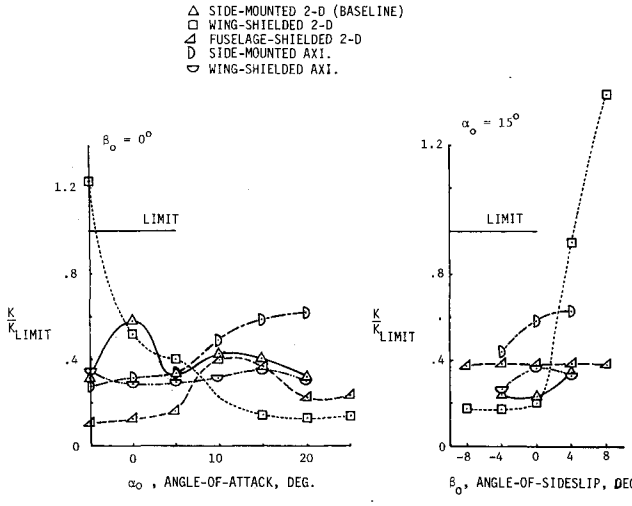

Fig. 16 Comparison of two-dimensional and axisymmetric inlet steady-state flow distortion; $M_0 = 2.2$.

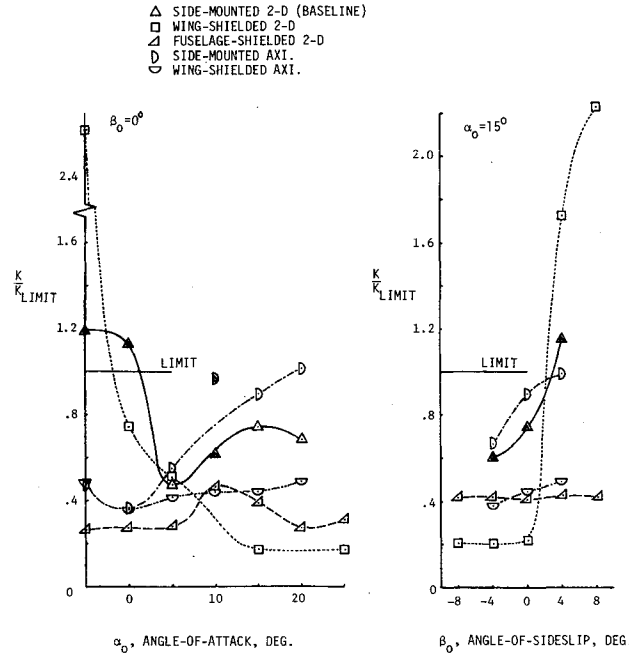

Fig. 18 Comparison of two-dimensional and axisymmetric inlet peak flow distortion; $M_0 = 2.2$.

pressor face steady-state flow distortion. Limit levels of distortion are exceeded in both cases. Otherwise, the only notable phenomenon is that the side-mounted, half-axisymmetric inlet reacts to high α_0 and positive β_0 with relatively high-flow distortion.

Flow Turbulence

The two-dimensional, wing-shielded inlet and side-mounted half-axisymmetric inlets exhibit sensitivities to flow angularity in terms of rms turbulence in Fig. 17 quite similar to their steady-state flow distortion tendencies. Here again, the parameter is high for the two-dimensional, wing-shielded inlet at negative α_0 and for both inlets at positive β_0. The only additional event is that the two-dimensional, side-mounted inlet flow also becomes noticeably more turbulent with positive β_0 (inlet on leeward side of aircraft).

Dynamic Flow Distortion

Finally, in Fig. 18, the time-variant nature of turbulent flow conditions is seen to be sufficient to push levels of dynamic distortion of two other inlets (half-axisymmetric side-mounted and two-dimensional side-mounted) above the limit level for various maneuver conditions at $M_0 = 2.2$. By way of contrast, the two-dimensional fuselage-shielded inlet and the half-axisymmetric wing-shielded inlet are notably low in dynamic distortion over the entire range of maneuver attitudes. Inlet-engine compatibility is shown to result from the proper combination of inlet configuration and placement.

Summary

Examination of diagnostic pressure data from the Tailor-Mate program has shown the following:

1) Performance degradation in wing-shielded and side-mounted two-dimensional leeward inlets is due to flow separation at the inboard sideplate in supersonic maneuvers.

2) Duct swirl exists in the side-mounted two-dimensional inlets, apparently due to duct offset and loft.

3) Performance is degraded in side-mounted half-axisymmetric inlets due to flow separation in the upper portion of the throat and resultant choking of the flow during supersonic maneuvers (both pitch and yaw angles).

4) Performance advantages are associated with fuselage shielding of two-dimensional inlets in supersonic maneuvering flight when considering the entire maneuver envelope.

5) Half-axisymmetric inlets exhibit performance advantages over two-dimensional inlets in the wing-shielded flowfield during supersonic maneuvering flight when considering the entire maneuver envelope.

6) Dynamic flow distortion measurement and sophisticated, high-speed analysis capability are shown to be important in the development of supersonic inlets for highly maneuverable aircraft.

References

[1]Cawthon, J.A., Truax, P.P., et al, "Supersonic Inlet Design and Airframe-Inlet Integration Program," AFFDL TR-71-124, Vols. I, II, and III, May 1973.

[2]Cawthon, J. A., Traux, P.P., and Savage, T.M., "Advanced Inlet Study (Tailor-Mate II)," AFFDL TR-73-72, June 1973.

[3]Surber, L.E. and Sedlock, D., "Analysis of Tailor-Mate Airframe-Inlet Flow Field Data and Inlet Performance Data for Supersonic Fighter Aircraft," AFFDL-TR-78-70, June 1978.

[4]Surber, L.E. and Stava, D.J., "Supersonic Inlet Performance and Distortion During Maneuvering Flight," AGARD CP 91-71, *Inlets and Nozzels for Aerospace Engines*, Dec. 1971.

[5]Surber, L.E., "Effect of Forebody Shape and Shielding Technique on 2-D Supersonic Inlet Performance," AIAA Paper 75-1183, AIAA/SAE 11th Propulsion Conference, Oct. 1975.

[6]Marous, J.J. and Sedlock, D., "Dynamic Data Editing and Computing System (DYNADEC)," *Proceedings of the AFSC Science and Engineering Symposium*, Kirtland AFB, New Mex., Oct. 1973.

[7]Sedlock, D., "Analog Screening of Tailor-Mate I .25 Scale Inlet Data Basic Configurations," Vols. I & II, AFFDL-TM-75-165-FXM, Dec. 1975.

[8]Sedlock, D., "Analog Screening of Tailor-Mate Alternate 2-D and 180 Half-Axisymmetric Side-Mounted and 2-D Wing Shielded Inlet Configuration," AFFDL TM-77-40-FXM, May 1977.